

# Gaseous surface hardening of martensitic stainless steels

**Tibollo, Chiara; Villa, Matteo; Christiansen, Thomas L.; Somers, Marcel A. J.**

*Publication date:*
2018

*Document Version*
Peer reviewed version

# Gaseous surface hardening of martensitic stainless steels

Chiara Tibollo, Matteo Villa, Thomas L. Christiansen, Marcel A. J. Somers

*Technical University of Denmark, Department of Mechanical Engineering, 2800 Kgs. Lyngby, Denmark, {chtibo, matv, tch, somers }@mek.dtu.dk*

**Abstract**

The present work addresses heat and surface treatments of martensitic stainless steel EN 1.4028. Different combinations of heat treatments and surface treatments were performed: conventional austenitisation, cryogenic treatment and in particular high temperature solution nitriding (HTSN) and low temperature surface hardening (LTSH). Controlled low temperature gaseous treatment was monitored with thermogravimetry. Reflected-light microscopy, X-ray diffraction and hardness-depth profiling were applied for the characterisation of the morphology and composition of the developing case. It was found that cubic lath martensite in conventionally austenitised EN 1.4028 dissolves nitrogen and develops expanded martensite (ferrite) during LTSH. HTSN leads to a microstructure of tetragonal plate martensite and retained austenite. The content of retained austenite can be reduced by a cryo-treatment and develops metastable expanded austenite during LTSH. Consistently, the case depth obtained after LTSH was shallowest after a prior cryo-treatment. Hardness values range up to 18 GPa after LTSH.

**Keywords**

Martensitic stainless steel, low temperature surface hardening, gas nitriding, hardness depth profile, X-ray diffraction

## 1 Introduction

Martensitic stainless steels are usually employed in applications where a combination of good corrosion resistance and strength are required, but they generally show poor fatigue and localized corrosion performance. In order to further improve the surface properties of these materials, surface engineering can be applied.

Traditionally, nitriding and nitrocarburising are considered bad practice for stainless steels, since the corrosion resistance relies on the availability of chromium in solid solution to maintain a passive layer, which is responsible for the corrosion protection. Nitriding, nitrocarburising and carburising under conventional conditions (typically between 490 °C and 950 °C) leads to the precipitation of chromium nitrides and/or carbides and impairs the corrosion properties, even though the surface hardness is improved. Hence, since the mid-1980s, the development of low-temperature surface hardening processes (below 440 °C) has received much interest [Christiansen, Somers 2013]. Low temperature surface hardening (LTSH) dissolves large quantities of nitrogen or carbon in the surface zone of the stainless steel while chromium is retained in solid solution, thereby avoiding nitride and/or carbide precipitation, and thus retain or even improve the localized (pitting and crevice) corrosion performance. A further improvement of wear resistance along with an increased pitting and crevice corrosion resistance is achieved by the formation of a supersaturated solid solution of nitrogen or carbon in austenite in the surface zone of the steel, while the fatigue performance could be improved by a compressive stress gradient below the surface. The supersaturated solid solution of interstitials in austenite or martensite is referred to as expanded austenite and expanded martensite, respectively. The dissolution of interstitials into stainless steels can be achieved by plasma and gaseous processes [Corengia et al. 2004, Frandsen, Christiansen, Somers 2006, Manova et al. 2006, Christiansen, Somers 2013]. A major advantage of gaseous over plasma-based processes is the possibility of straightforward thermodynamic control and monitoring of the gas composition, enabling accurate tailoring of the hardened case. The main complication in gaseous thermochemical

treatments lies in by-passing the passive film on the surface of the stainless steel [Somers, Christiansen 2015b]. Therefore, surface activation is necessary to remove or transform the passive layer [Somers, Christiansen 2015a]. Low temperature surface hardening relies on kinetically preventing the development of nitrides/carbides by choosing the treatment time shorter than the incubation time for nitrides/carbides.

A second possibility for improving the performance of martensitic stainless steels by surface engineering is dissolving nitrogen at temperatures beyond the thermodynamic dissolution temperature of chromium nitrides/carbides, so-called high temperature solution nitriding (HTSN), hence yielding surface hardening while avoiding the precipitation of chromium nitrides. Ideally, after quenching the result of HTSN is a case of nitrogen martensite with an underlying core of carbon-rich martensite. A consequence of dissolving nitrogen is a reduction of the martensite start temperature, which eventually could imply that (part of the) austenite is retained in the case, which could necessitate an additional cooling treatment to sub-zero temperature (cryogenic treatment) to transform austenite to martensite.

Because of the improvement of corrosion resistance due to the presence of nitrogen and a case hardness in the range of 7–8.5 GPa, HTSN can be considered a separate thermochemical surface hardening treatment. Moreover, HTSN can be succeeded by a LTSH treatment for further improvements in surface hardness and localized (pitting and crevice) corrosion performance. If necessary, a cryogenic treatment could be an intermediate step in-between HTSN and LTSH. In the present contribution the combinations of LTSH, HTSN and cryogenic treatment are investigated for EN 1.4028 (AISI 420F).

# 2 Experimental

## 2.1 Material and sample preparation

The alloy investigated was a commercial EN 1.4028 (AISI 420F) with composition given in Table 1. The carbon content was determined with a LECO CS230 combustion analyser. The steel was delivered as a Ø10 mm bar in as-rolled condition. Samples were 3-mm-thick discs, which were cut into quarters and ground and polished up to 4000 paper. Finally, the samples were cleaned in ethyl alcohol.

| | **Cr** | **C** | **Mn** | **Si** | **P** | **S** | **Fe** |
|---|---|---|---|---|---|---|---|
| *Wt%* | 13 | 0.45 | 1.3 | 0.8 | 0.03 | 0.01 | balance |

Table 1: Chemical composition of the alloy employed

Two different process routes of heat and surface treatments were followed. A conventional process route, where Low Temperature Surface Hardening (LTSH) was applied after conventional austenitisation treatment (CONV) and an, optional, cryogenic treatment (CRYO). The other process route entailed High Temperature Solution Nitriding (HTSN), optionally followed by cryogenic treatment (CRYO) and finally LTSH. An overview of the different treatment combinations is given in Table 2.

Conventional austenitisation was performed for 1 h at 1040 °C in a horizontal furnace with continuous gas flow of 0.4 l/min of argon in order to avoid oxidation. The HTSN treatment was performed in the same furnace as for austenitisation, for 2 h at 1110 °C with a continuous flow of 1.2 l/min of nitrogen at a pressure of 1 bar. For both treatments cooling to room temperature occurred at an average cooling rate of 40 °C/min. Cryogenic treatment of the samples was performed for 24 h at the sublimation temperature of dry ice, i.e. –78 °C. The LTSH treatment was performed by gaseous nitriding in a Netzsch STA 449 F3 Jupiter thermal analyzer at 420 and 400 °C for 16 h in a gas mixture of $NH_3$ and $H_2$. The LTSH treatment starts with a proprietary in-situ surface activation, followed by a 1 h treatment in pure $NH_3$ (100 ml/min) and 15 h treatment in 50 ml/min of $NH_3$ and 50 ml/min of $H_2$. During all treatments in the thermal

analyzer, a continuous flow of 8 ml/min, corresponding to 8 % of nitrogen was applied for protection of the electronics in the instrument.

| | CONV | HTSN | CRYO | LTSH | Designation |
|---|---|---|---|---|---|
| CONV SERIES | I | | | | CONV |
| | I | | II | | CONV+CRYO |
| | I | | | II | CONV+LTSH |
| | I | | II | III | CONV+CRYO+LTSH |
| HTSN SERIES | | I | | | HTSN |
| | | I | II | | HTSN+CRYO |
| | | I | | II | HTSN+LTSH |
| | | I | II | III | HTSN+CRYO+LTSH |

Table 2: Order of followed treatments and naming of the samples

## 2.2 Materials characterisation

After each treatment, cross sections of the samples were prepared for metallographic investigation. Hot mounting at 180 °C and 20 kN for 3 min, followed by grinding and polishing were performed, with a final polishing step (after diamond polishing up to 1 μm) in a colloidal silica suspension. Various etching techniques were applied for the samples: Kalling's II, Murakami, HCl-modified Nital, at different dilutions. Because of the heterogeneity of the microstructures finding the right (combination of) etchants was elaborate. Reflected light microscopy was performed with Olympus GX 41 and Zeiss Neophot 30 microscopes. Vickers hardness measurements were performed on un-etched samples using a Future-Tech FM-700 and a DuraScan-70 micro-hardness testers, applying a load of 10 g for a dwell time of 10 s.

For phase identification X-ray diffraction analysis was performed using a Bruker D8 Discovery X-ray diffractometer, equipped with Cr $K_\alpha$ radiation. Diffractograms were recorded in symmetrical θ–2θ scans in parallel beam geometry from 40 to 160 °2θ with a step-size of 0.06 °2θ and a measurement time of 8.7 s per step.

# 3 Results and discussion

## 3.1 Conventional series

Reflected light micrographs of the cross sections of LTSH-treated samples in the conventional hardening series are given in Figure 1, while the corresponding X-ray diffractograms are presented in Figure 2. XRD shows that conventional hardening leads to a predominantly martensitic structure with a small fraction of retained austenite, which after cryogenic treatment is further reduced (Figure 2a). Small peaks emerging from the background at 58, 64, 75 and 80 °2θ originate from the presence of carbides in the steel, which inidicates that the conventional treatment does not dissolve all carbides. As no tetragonality of the martensite is observed in the CONV and CONV+CRYO diffractograms, the carbon content in martensite is low, consistent with the very low fraction of retained austenite, indicating that martensite is of lath type and the presence of carbides in the cross sections in Figure 1. Apparently, at the conventionally chosen austenitisation temperature no complete dissolution of the carbides occurs, probably because of the relatively high carbon content of 0.45 wt.% for this alloy, as compared to the usual content of about 0.20 wt.% for EN 1.4028 (AISI 420) grades. ThermoCalc calculations confirmed that for the alloy composition $M_7C_3$ carbides are stable at the chosen austenitisation temperature. The hardness values determined over the thickness of the CONV and CONV+CRYO samples (see

average values represented by coloured full symbols in Figure 3) are equal within experimental accuracy, but a slightly higher average hardness value was measured after cryogenic treatment. LTSH leads to the appearance of a zone in the cross section (Figure 1a) and a shoulder in the diffractogram (Figure 2a). The shoulder is identified as expanded martensite ($\alpha'_N$) and the precipitation of CrN. The dissolution of nitrogen into pre-existing martensite (essentially this is ferrite) is not accompanied by tetragonality, but rather an expansion of the cubic lattice. This is explained from the fact that no actual martensitic transformation is involved, rather short-range ordering of Cr and N governs the distribution of the N atoms. Apparently the nitrogen content is too low to stabilise the development of (expanded) austenite. Also, small peaks emerge at 63 and 74 °2θ in Figure 2a, which hint at the development of $Fe_4N$ nitrides. The effect of a cryogenic treatment in-between conventional hardening and LTSH appears to lead to a stronger peak of expanded martensite and CrN (Figure 2b), while both the micrograph in Figure 1b and the hardness profile in Figure 3 suggest a shallower case depth.

From the results of the CONV series the following picture emerges. The dissolution of nitrogen during LTSH leads to the development of expanded martensite and the precipitation of CrN nitrides. Also, partial transformation of the originally present carbides into nitrides is expected. Evidently, the duration of the LTSH treatment has been too long or the temperature was too high to prevent the formation of CrN. For comparison, a similar treatment of austenitic stainless steel (with a high chromium content and nickel to stabilise austenite) does not lead to CrN precipitation under the chosen nitriding conditions (cf. [Somers, Christiansen 2015b]. It is well established that the nucleation of CrN is promoted in b.c.c. (cubic martensite) because of the favourable Baker-Nutting orientation relationship [Somers, Lankreijer, Mittemeijer 1989].

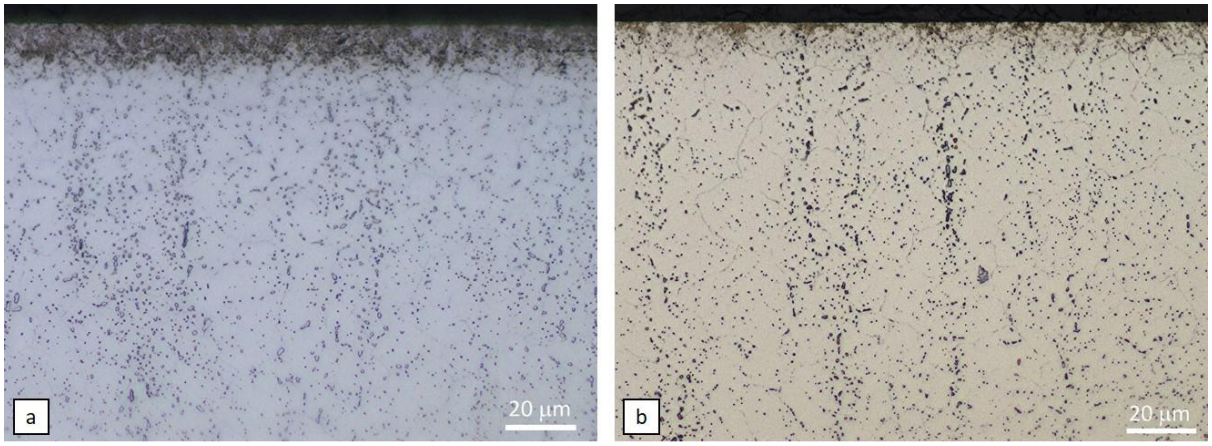


Figure 1: Reflected light micrographs showing the microstructure of samples CONV and CONV+LTSH. Etching with Murakami and HCl-modified Nital.

The more abundant $\alpha'_N$/CrN peak and the shallower case depth after LTSH of a cryogenically treated sample is explained as follows. During cryogenic treatment, the austenite to martensite transformation progresses. Continued transformation of austenite into martensite leads to an increase in the number of crystallographic defects, such as dislocations, in both martensite and retained austenite [Christien, Telling, Knight 2013]. Defects in martensite act as nucleation sites for precipitation of CrN during LTSH. Evidently in the present case the cryo-treatment has lead to the availability of many nucleation sites for CrN precipitation. The precipitation of CrN leads to binding of nitrogen and the possible containment of excess nitrogen [Somers, Lankreijer, Mittemeijer 1989, Schacherl, Graat, Mittemeijer 2004]. The total solubility thus achieved is higher than the maximum solubility in expanded martensite, which was previously demonstrated to be about 10 at.%N. Consequently, less nitrogen will diffuse to larger depth and a shallower case depth results. The maximum hardness reached, adjacent to the surface, is about 17 GPa, which is appreciably higher than for expanded austenite, which reaches about 12 GPa.

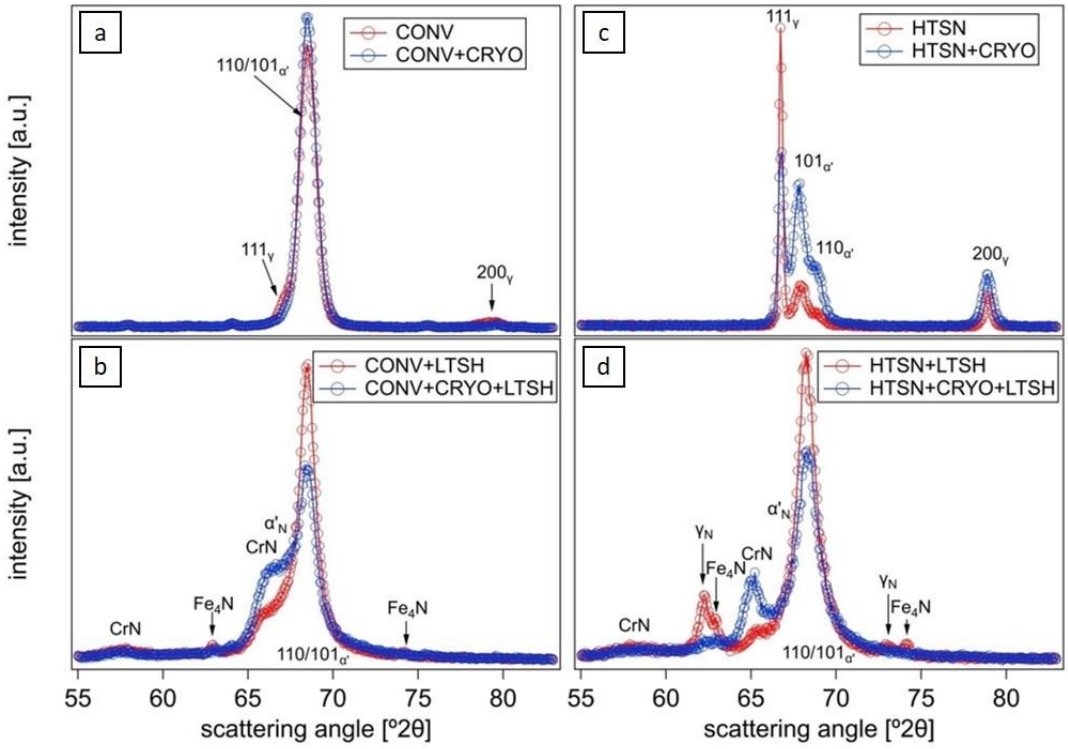


Figure 2: X-ray diffractograms for the various treatments.

## 3.2 High temperature solution nitriding series

Reflected light micrographs of the cross sections of LTSH-treated samples in the HTSN-treated series are given in Figure 4, while the corresponding X-ray diffractograms are presented in Figure 2. XRD shows that HTSN-treatment leads to tetragonal martensite with a large fraction of retained austenite, which after cryogenic treatment is importantly reduced (Figure 2c). Evidently, martensite formation from nitrogen (and carbon)-containing austenite, leads to tetragonality. As compared to the conventionally hardened series no peaks hint at the presence of carbides in the steel; neither were nitride peaks identified. This inidicates that all carbides were dissolved and that no nitrides developed at the HTSN temperature (in accordance with ThermoCalc calculæations (not included)) or during cooling. The microstructures in the bulk in Figure 4 are consistent with the XRD results: plate martensite is present in both samples and the fraction of retained austenite is appreciably lower for the cryo-treated sample. It is expected that the fraction of austenite is highest at the surface, because the nitrogen content is highest in this region. The hardness values determined over the thickness of the HTSN and HTSN+CRYO samples (see average values represented by coloured symbols in Figure 3) show that the increase in martensite content in the bulk on cryo-treatment is accompanied by a hardness increase in the core. The large standard deviations reflect the heterogeneity of the martensite/austenite microstructure and the low load used for hardness measurement.

LTSH leads to a complicated microstructure at the surface: a dark zone appears in the outer 20 µm for the HTSN+LTSH sample and white patches within. This dark zone is not as pronounced for the LTSH+CRYO+HTSN sample, and it appears that the martensite plates do not become dark during etching. X-ray diffraction analysis after LTSH (Figure 2d) shows that the tetragonality of martensite disappears, i.e. martensite is tempered, that austenite is removed and that both CrN and $Fe_4N$ develop. Also expanded austenite ($\gamma_N$) was identified, which is considered to develop from retained austenite. The lowest fraction of expanded austenite was found in the cryo-treated sample, consistent with the lower retained austenite content.

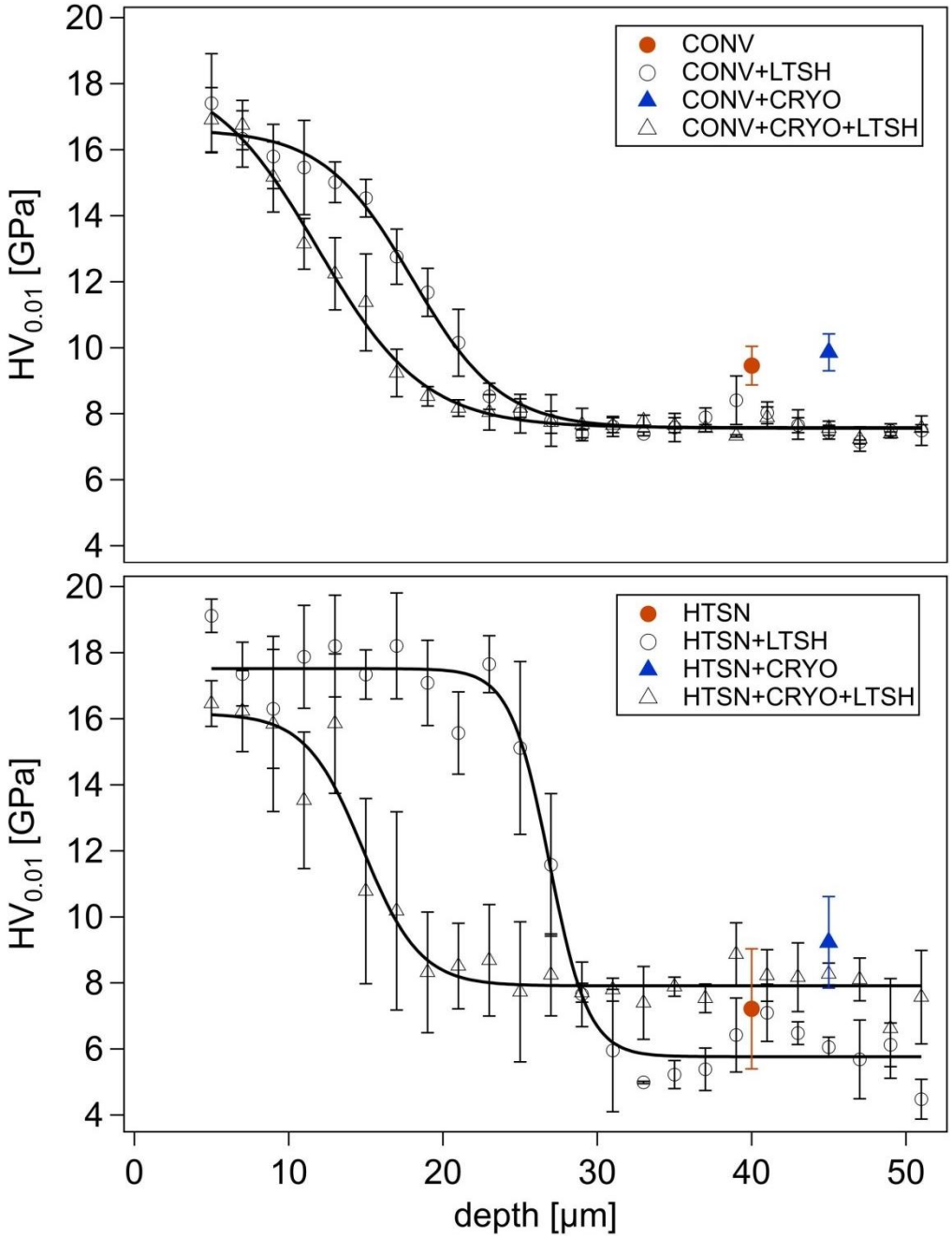


Figure 3: Hardness depth profiles for the various treatments.

From the results from the HTSN series the following picture emerges. For the HTSN+LTSH sample, which contains a high fraction of retained austenite, the case developing at the surface is expected to contain mostly expanded austenite, with regions of expanded martensite. Evidently, the expanded austenite is decomposing into ferrite and $CrN/Fe_4N$, which explains the disappearnce of the austenite peak. Even though the case in the HTSN+LTSH sample shows features that hint at decompased plate martensite, it appears that tempered and (possibly) expanded martensite is more stable against decomposition that expanded austenite. The reason that expanded austenite is unstable as compared to expanded austenite forming on austenitic stainless steel is the absence of the austenite stabilising element Ni. Nevertheless the retained austenite in the bulk does not decompose during the 16 h LTSH treatment.

The shallower case depth in the cryo-treated sample is even more pronounced for the HTSN series than for the CONV series (cf. Figure 1b and 4b). This is likely to be associated with the content of retained austenite. However, the solubility of nitrogen is higher in expanded austenite than in expande martensite and the nitrogen diffusion proceeds faster through martensite than

through austenite. The cause for the shallower case depth after intermediate cryo-treatment reamins therefore unclear, and needs further investigation.

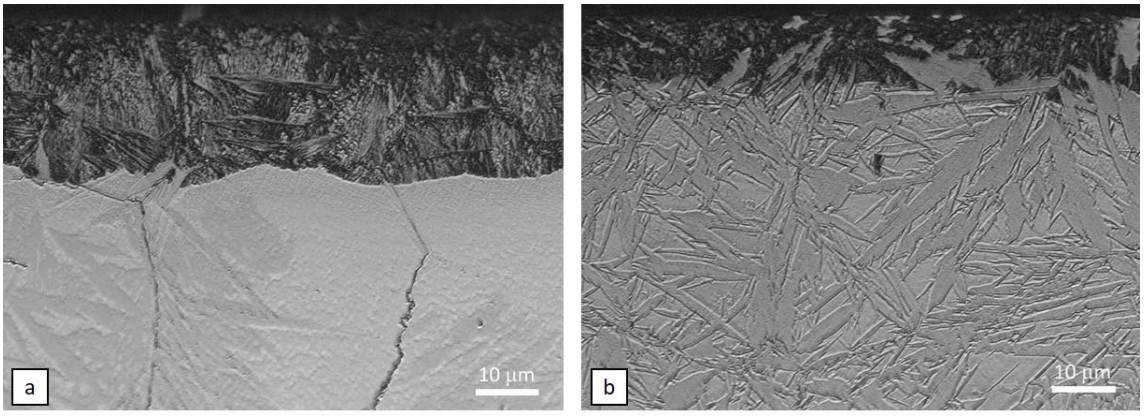


Figure 4: Reflected light micrographs showing the microstructure of samples HTSN+LTSH and HTSN+CRYO+LTSH. Etching with Murakami and HCl-modified Nital.

## 4 Conclusions

Martensitic stainless steel EN 1.4028 can be thermochemcially treated by high temperature solution nitriding (HTSN) at 1110 °C in $N_2$ and low temperature surface hardening (LTSH) at 420 °C in $NH_3$. Conventional austenitising leads to lath martensite, which dissolves nitrogen during LTSH and forms expanded martensite. HTSN leads to plate martensite and retained austenite. Cryo-treatment reduces the retained austenite content importantly. LTSH of HTSN treated samples leads to metastable expanded austenite which decomposes into ferrite and $CrN+Fe_4N$ during treatment. Irrespective of the austenitisation, a cryo-treatment before LTSH reduces the case depth. The micro hardness after LTSH is enhanced to 16–18 GPa by a low temperature surface hardening treatment.

**Acknowledgement**

The authors are grateful to Institut de Recherche Technologique Matériaux, Métallurgie et Procédés (IRT-M2P Metz, France) for financial support for the current research activities.

**References**

Christiansen, T. L. and Somers, M. A. J. (2013) 'Low-Temperature Surface Hardening of Stainless Steel', *Advanced Materials & Processes*, (November-December), pp. 52–53.

Christien, F., Telling, M. T. F. and Knight, K. S. (2013) 'Neutron diffraction in situ monitoring of the dislocation density during martensitic transformation in a stainless steel', *Scripta Materialia*. Acta Materialia Inc., 68(7), pp. 506–509. doi: 10.1016/j.scriptamat.2012.11.031.

Corengia, P. *et al.* (2004) 'Microstructure and corrosion behaviour of DC-pulsed plasma nitrided AISI 410 martensitic stainless steel', *Surface and Coatings Technology*, 187(1), pp. 63–69. doi: 10.1016/j.surfcoat.2004.01.031.

Frandsen, R. B., Christiansen, T. and Somers, M. A. J. (2006) 'Simultaneous surface engineering and bulk hardening of precipitation hardening stainless steel', *Surface and Coatings Technology*, 200(16–17), pp. 5160–5169. doi: 10.1016/j.surfcoat.2005.04.038.

Manova, D. *et al.* (2006) 'Influence of annealing conditions on ion nitriding of martensitic stainless steel', *Surface and Coatings Technology*, 200(22–23 SPEC. ISS.), pp. 6563–6567. doi: 10.1016/j.surfcoat.2005.11.035.

Schacherl, R.E.; Graat, P.C.J.; Mittemeijer, E.J.: The nitriding kinetics of iron-chromium alloys; the role of excess nitrogen: experiments and modelling, Metall. Mater. Trans. A, vol. 35A, 2004, pp. 3387-3398.

Somers, M. A. J. and Christiansen, T. L. (2015a) 'Gaseous processes for low temperature surface hardening of stainless steel', in Mittemeijer, E. J. and Somers, M. A. J. (eds) *Thermochemical Surface Engineerinf of Steels*. Woodhead Publishing, Elsevier, pp. 581–614. doi: 10.1007/978-3-319-21533-4.